PCIM Europe Digital Days 2021

Improved Natural-Air-Convection-Cooling Formulas for Medium Frequency Transformer Design Optimization

J. L. Roy, M. Mogorovic, and D. Dujic

POWER ELECTRONICS LABORATORY
ÉCOLE POLYTECHNIQUE FÉDÉRALE DE LAUSANNE

Improved Natural-Air-Convection-Cooling Formulas for Medium Frequency Transformer Design Optimization

Jonas Le Roy, Marko Mogorovic, Drazen Dujic

Power Electronics Laboratory (PEL), École Polytechnique Fédérale de Lausanne (EPFL), Switzerland

Corresponding author: Jonas Le Roy, jonas.l.roy@gmail.com

Abstract

This paper provides accurate analytic models for a computationally efficient estimation of the natural convection cooling coefficients for typical geometries, such as those encountered in transformers. Proper thermal coordination is an essential step of any transformer design, especially when it comes to medium frequency operation, where the cooling surfaces are greatly reduced due to the frequency scaling. Available empirical formulas, derived for simple geometries, have a limited applicability to such complex structures. In this work, analytic models are derived based on extensive finite element method simulations that accurately describe the convective heat transfer of the geometries of interest. The proposed models improve accuracy substantially compared to the available models and have several orders of magnitude faster execution referred to finite element method simulations.

1. Introduction

With the increase of the renewable and decentralized production of energy, the medium voltage DC (MVDC) power distribution has been gaining popularity in recent years. High-power medium-voltage DC-DC converters are needed to enable the MVDC networks [1], and also in support of various other applications such as railway and e-mobility [2], [3]. A medium frequency transformer (MFT) is needed to provide galvanic isolation and input-output voltage matching in such a converter. The MFT size can be significantly decreased due to a high operating frequency, enabled by modern semiconductors. Consequently, cooling conditions in MFTs are more difficult. Therefore, adequate modeling is needed in order to perform a correct thermal coordination and to properly utilize the available cooling channels, integrated into design.

Thermal modeling can be approached with the numerical finite elements method (FEM). While FEM generally offers precise results for all kinds of geometries and boundary conditions, there are several disadvantages of this approach that are especially limiting in case of complex multiphysics processes, such as convection. In contrast to conduction and radiation, convection is a rather complex process that features both heat and mass transfer. Computational fluid dynamics (CFD) FEM calculations are extremely challenging. Correct meshing, setup of the solution domain, convergence issues and oscillations in the steady state make it difficult to extract reliable solutions for convection problems. Moreover, the computational cost is extreme, even for simple geometries. Finally, the training and time needed to properly setup the CFD FEM model of the MFT is not negligible.

Due to convergence issues and a high computation cost tied to FEM, especially for complex multiphysics processes such as convection [4], thermal modeling is often performed using the equivalent electric circuit representation (i.e. thermal network) that utilizes simple empirical analytic formulas to describe the equivalent conduction, convection and radiation thermal resistances [5], [6], [7]. While this method provides a relatively simple and computationally efficient modeling alternative, it is tied to various assumptions and geometry simplifications, that may have a significant impact on the modeling accuracy. An example of a detailed an-

ISBN 978-3-8007-5515-8

alytic approach to thermal modeling, can be found in [8]. An MFT prototype has been built to verify the analytic thermal model. Higher hot-spot temperatures than expected were reported, especially within the windings. According to the analysis and conclusions from [8], this discrepancy can be attributed to the poor quality of the calculated natural convection thermal resistances within the thermal network. Namely, radiation and conduction are relatively well understood, and thereby no major simplifications in MFT geometry had to be made for existing formulas. However, to take convection into account, empirical formulas were used that describe the convection cooling of a hot plate with constant temperature in quiescent air, while convection coefficients are highly dependent on both the geometry of the cooling surface and any other surrounding objects that may influence the fluid flow. This was shown to be an oversimplified representation for the given complex geometry setup, especially in the case of the transformer windings whose surfaces are separated from other objects by very small air clearances and are partially located within the semi-enclosure of the core window.

In regard to the aforementioned modeling challenges, this paper provides analytic models for a fast estimation of the natural air convection coefficients for typical geometries, such as encountered in transformers. By combining the flexibility of CFD FEM modeling with the simplicity of analytic equations, using a data driven approach [9], [10], a more accurate analytical description of natural convection is achieved, and verified on a custom built experimental setup. With the improved analytical models for convection processes in MFTs, a simple and sufficiently accurate analytical set of models are made available for a proper thermal design of MFTs.

2. Modeling Methodology

Full CFD FEM modeling of complex geometries, such as MFTs, features extreme computational cost, problems with numeric stability and dependency on various model settings, thus, as shown in [4], the results can only be used for quantitative interpretation.

Instead of a full 3D FEM analysis of different MFTs, symmetry and knowledge of the underlying physics is used to partition the geometry of interest and derive simple details that provide a good representation of the convection cooling behavior of the entire MFT. These details can still be relatively efficiently solved with CFD FEM. Data collection is fast and inexpensive compared to the real experiment. With the extracted results, analytic formulas are developed for convection cooling, which take MFT geometry into account.

The MFT structure is first simplified to a 3D representation, as illustrated in Fig. 1. For the outer surfaces of the part of the windings out of the magnetic core, the equation describing convection for a vertical plate in free air can still be used. As regards to the inner surfaces of the part of the windings out of the magnetic core (facing another winding or magnetic core), convection cooling will be influenced by the small air gap between the windings or winding and the core.

Parallel plates with distance d, illustrated in Fig. 2a, will serve as a geometry to estimate the influence of the gap between the windings on convection cooling. A plate in a semi-enclosure, as shown in Fig. 2b, will serve as a model to obtain insight in convective cooling of the portion of the windings within the magnetic core. Parallel plates and a plate in a semi-enclosure will be called model 1 and 2, respectively.

Due to the similarity between models 1 and 2 and a vertical plate in free air, the convection coefficients of models 1 and 2 are normalized to the respective convection coefficients of a vertical plate in free air, calculated by the empirical equation for the laminar

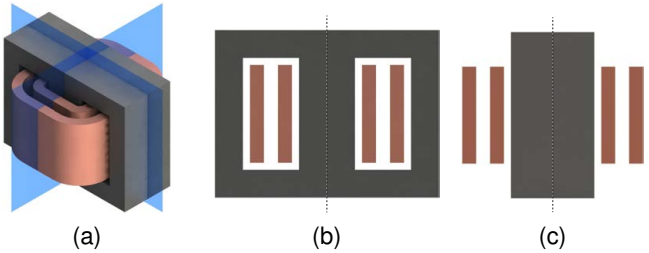

Fig. 1: (a) 3D MFT structure with highlighted thermal planes of symmetry; (b) 2D symmetry detail capturing the geometry within the core window; (c) 2D symmetry detail capturing the geometry outside of the core window [8].

ISBN 978-3-8007-5515-8

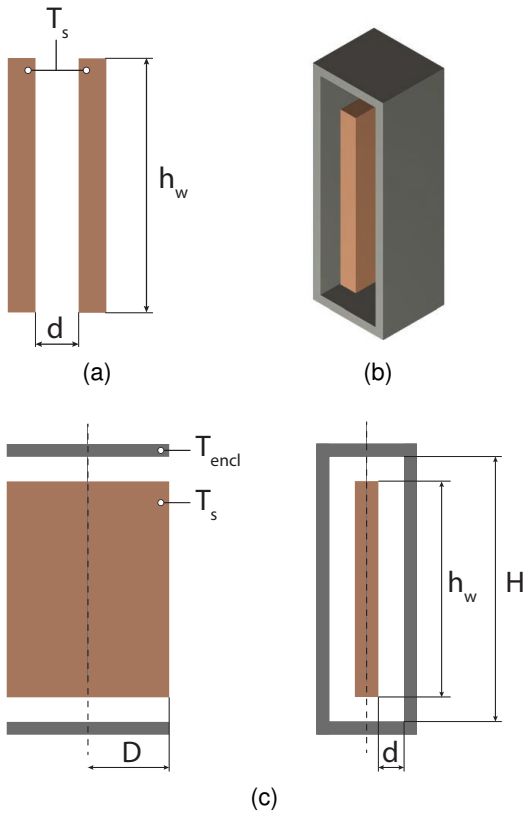

Fig. 2: Simplified geometries of interest: (a) model 1 - two parallel hot plates in free air; (b) model 2 - hot plate in semi-enclosure; (c) cross sections of model 2.

convection cooling of a plate in free air:

$$\overline{h} = \frac{k}{L}\{0.68 + \frac{0.670Ra^{1/4}}{(1+(0.492/Pr)^{9/16})^{4/9}}\} \quad (1)$$

as presented in [11]. For the geometry and temperature range of interest in MFT applications, Rayleigh numbers show that the airflow can be considered laminar. Therefore, formulas are derived that serve as a correction factor for the convection coefficients of a hot plate in free air, as calculated with (1).

In order to verify the used CFD FEM model settings, simulations on a model of the hot plate in free air have been performed, as a control case, and compared to the results of (1). A plate with length L and small width is modeled with 2D CFD FEM with constant temperature T_s on the plate side surfaces and ambient air temperature T_∞. For those boundary conditions, the total heat transfer flux Q is calculated via integration of the local heat flux q" over the plate surface. Knowing the temperature difference and the surface of the plate, calculation of the

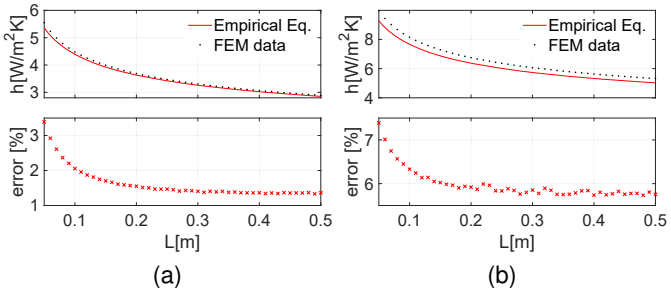

Fig. 3: Natural convection coefficients of a vertical plate in free air plotted against plate length L, derived from CFD FEM models (black) and calculated with empirical formula (1) (red): (a) $\Delta T = 10K$; (b) $\Delta T = 120K$.

mean convection coefficient $\overline{h}$ is done via (2).

$$\overline{h} = \frac{\frac{1}{A}\int_A q"dA}{T_s - T_\infty} \quad (2)$$

Targeted sample simulations were performed and it was confirmed that the influence of T_∞ for same temperature differences ΔT is negligible within the range of interest - with $\overline{h}$ errors less than 3% within a wide T_∞ range $[15, 70]°C$. Therefore, $\overline{h}$ is assumed to be dependent on only two variables for our range of interest. Plate lengths from $0.05m$ to $0.5m$ and temperature differences from $10°C$ to $120°C$ are considered, as they represent the winding conditions encountered in MFTs. 1058 2D CFD FEM simulations, with varying parameters within the aforementioned ranges of interest, were performed for a vertical plate in free air.

For the sake of illustration, sample CFD FEM simulation results are provided in Fig. 4a and b. As shown in Fig. 3, natural convection coefficients of a vertical plate, derived from CFD FEM models, are compared with their corresponding values, calculated with empirical formula (1). As can be seen, the FEM results are within the expected range, follow a similar curve and have little to no dispersion. Differences between (1) and FEM data are in range of those, caused by imperfections of the experimental setup and measurement.

Results are in expected range, have little dispersion and errors are well below 10%. This confirms the fidelity of the realized CFD FEM modeling setup and justifies its use on the two aforementioned geometry details - model 1 and 2.

ISBN 978-3-8007-5515-8

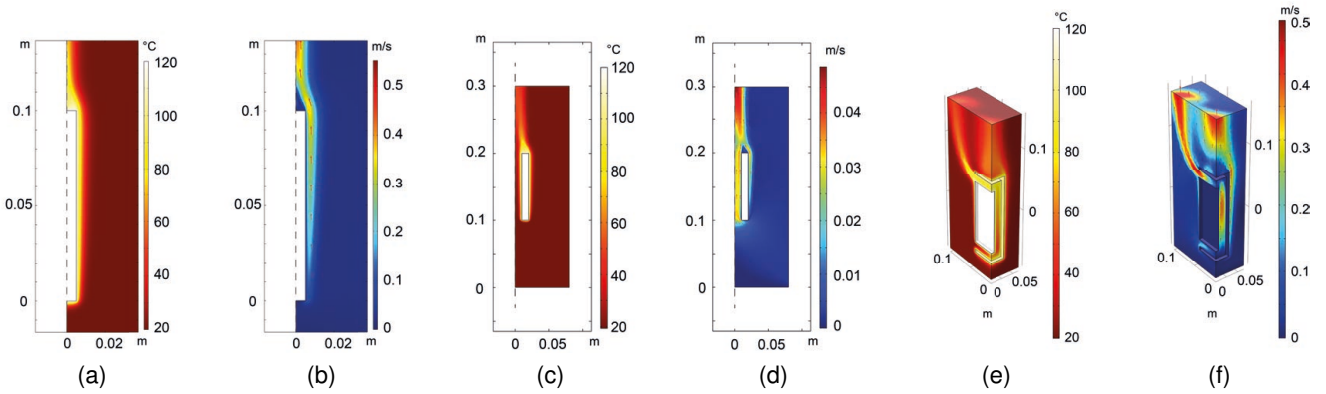

Fig. 4: CFD FEM sample results: (a) temperature profile of a hot vertical plate in free air; (b) velocity profile of a hot vertical plate in free air; (c) temperature profile of model 1; (d) velocity profile of model 1; (e) temperature profile of model 2; (f) velocity profile of model 2.

3. Development of Multivariable Models

As explained earlier, analytic equations are developed for the normalized correction functions

$$f_{c1} = f_1/f_{plate} \quad \text{and} \quad f_{c2} = f_2/f_{plate} \tag{3}$$

for model 1 and 2, respectively. f_{c1} and f_{c2} represent the analytic equations in form of a correction formula for (1), that take into account the air gap width and the geometry of the semi-enclosure, respectively. f_1 and f_2 represent the absolute average convection values obtained from the FEM data, for model 1 and 2, respectively. f_{plate} represents the average convection coefficients calculated with (1).

3.1. Model 1 - Two parallel hot plates in free air

As illustrated in Fig. 2a, f_{c1} is a function of the air gap width d, the temperature difference ΔT, and the height of the winding h_w. In order to provide the necessary data, sweeps of d are done with 27 combinations of ΔT and h_w, resulting in about 800 simulations of model 1 within the range of interest. The 800 simulations are a trade-off between total required calculation time and accuracy of the resulting curve fit. For the sake of illustration, sample results of CFD FEM simulations are provided in Fig. 4c and d.

The considered ranges of ΔT and h_w are $10K$ to $120K$ and $0.05m$ to $0.5m$, respectively, as they represent typical MFT boundary conditions. For the sake of illustration, in Fig. 5a, plots of h against d are made with ΔT and h_w having extreme values of the range of interest. As curves have a maximum for a specific d, a chimney effect is present - i.e. the presence of a hot surrounding geometry can influence convection cooling positively. As illustrated in Fig. 6, for certain values of d, the interaction of the temperature boundary layers result in greater air density differences, that increase the air velocity between the two plates.

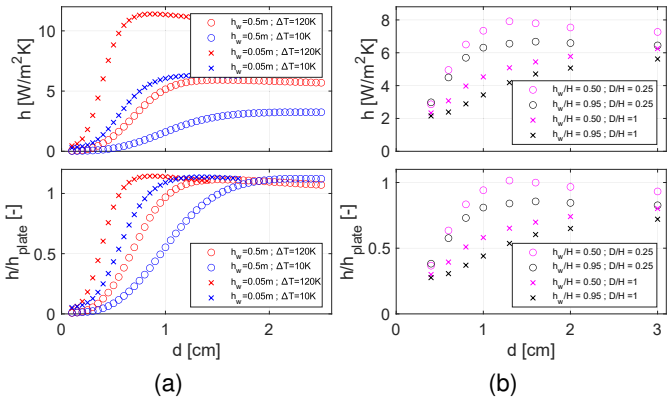

Fig. 5: Curves resulting from CFD FEM sweeps, representing absolute and normalized natural convection coefficients as a function of d (a) for the natural convection cooling of the inner side of parallel plates in free air for boundaries range of interest h_w and ΔT ; (b) for the natural convection cooling of a plate in a semi-enclosure, where x_2 and x_3 are equal to the range of interest and x_4 = 80%.

For model 1, a correction formula is derived using

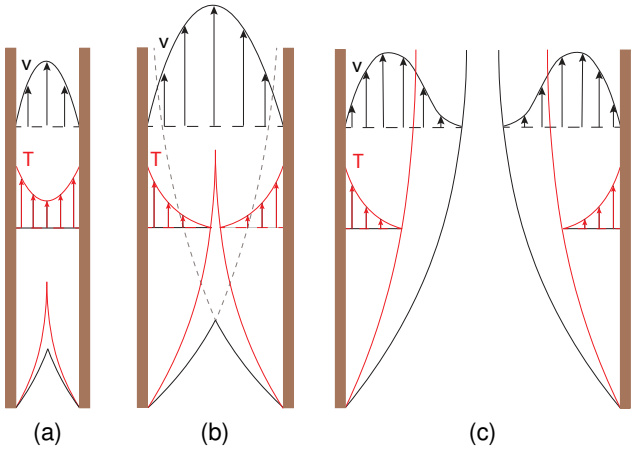

Fig. 6: Small values of d: (a) negative interaction between temperature and velocity boundary layers; (b) chimney effect: positive interaction between velocity boundary layers; (c) no interaction between temperature and velocity boundary layers.

curve fitting, based on the acquired FEM results:

$$f_{c1}(d, \Delta T, h_w) = e^{-12.715e^{-kd}+0.28833e^{-55.593d}} \tag{4}$$

where

$$k = 1344.7h_w^2 - 1297.8h_w - 0.017258\Delta T^2 + 3.3679\Delta T + 570.99 \tag{5}$$

where d and h_w are expressed in $[m]$ and ΔT in $[K]$.

For the sake of illustration, three sample curves of the proposed correction factor model are plotted in Fig. 7a, and are compared with their corresponding CFD FEM data. The proposed equation has typical relative errors below 2% in range from $0.8cm$ to ∞. For values of d lower than $0.8cm$, while still very well following the curve, higher relative estimation errors, up to 80%, can be expected due to the very low absolute values of the convection coefficients.

It can be concluded that the proposed correction model (4) drastically improves the accuracy of convection formulas, compared to the single plate empirical model, especially for low ranges of d (several orders of magnitude).

3.2. Model 2 - hot plate in semi-enclosure

Model 2 is fully defined by 11 multi-physics variables. Despite all the iteratively achieved model optimizations (e.g. domain, mesh and solver), 3D

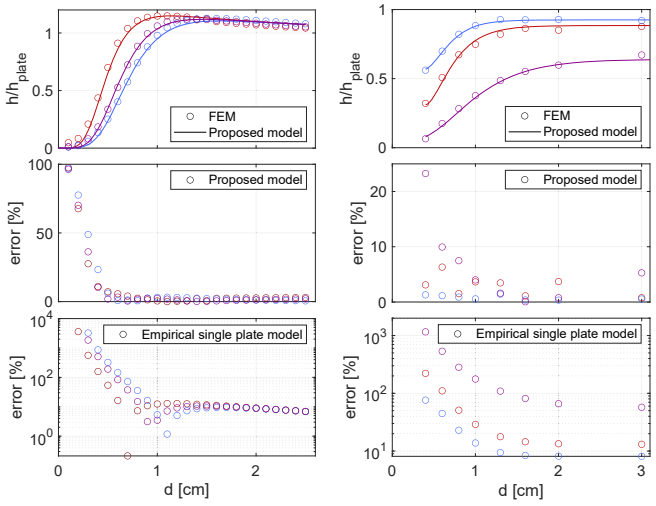

Fig. 7: Top: comparison between proposed multivariable model and the acquired FEM data. Middle: the error of the proposed model compared to FEM. Bottom: the error of the empirical single plate model compared to the proposed model: (a) 3 sample curves against d for model 1; (b) 3 sample curves against d for model 2.

CFD FEM simulations needed for the geometry of model 2 remain extremely computationally intensive. Based on the results of targeted test simulations, the effect of certain variables has been proven practically negligible (errors below 5%, thus allowing a reduction of the dimension of the model). It is shown that convective cooling can be analyzed by the following four normalized variables: d, D/H, h_w/H and $\Delta T_{encl}/\Delta T \cdot 100\%$, where, as illustrated in Fig. 2c, d represents the clearance between the winding and inner side enclosure, D represents the enclosure depth, H represents the inner height of the enclosure, h_w represents the winding height, ΔT_{encl} represents the temperature difference between the enclosure and ambient, and ΔT represents the temperature difference between winding and the ambient. The four significant variables and their ranges are summarized in Tab. 1.

As a result of careful selection and discretization of the relevant variables, the total amount of simula-

Tab. 1: Declaration of the variables used for model 2.

Vars.	$x_1[m]$	$x_2[-]$	$x_3[-]$	$x_4[\%]$
Def.	d	D/H	h_w/H	$\frac{\Delta T_{encl}}{\Delta T}100\%$
Range	$[0.004, 0.03]$	$[0.25, 1]$	$[0.5, 0.95]$	$[60, 100]$

tions is limited to 864, which was still a reasonable number of simulations for a cluster of six (i5 8Gb RAM) computers, lasting roughly 10 days. For the sake of illustration, sample CFD FEM simulation results are provided in Fig. 5e and f.

While only 32 out of the 864 simulations are displayed (as a dot) in Fig. 4b, important conclusions can be derived from these plots. Firstly, the influence of D/H is more profound than h_w/H. Secondly, a chimney effect is still present in model 2, but less distinct compared to the effect in model 1. Lastly, as expected, for very small values of d and $x_4 \neq 100\%$, instead of converging to zero, the curves are dominated by the effect of conduction between the hot plate and semi-enclosure through a thin layer of quasi-static air.

Again, a correction formula is derived and its coefficients calculated via curve fitting, based on the acquired CFD FEM data for model 2:

$$f_{c2}(x_1, x_2, x_3, x_4) = C_1 e^{-C_2 e^{-C_3 x_1} + C_4 e^{-C_5 x_1}} \tag{6}$$

where the vector **C** accounts for the dependency on x_2, x_3 and x_4:

$$\begin{bmatrix} C_1 \\ C_2 \\ C_3 \\ C_4 \\ C_5 \end{bmatrix} = \begin{bmatrix} -0.26767 & -0.27233 & -0.00074558 \\ -7.2550 & 0.43605 & 0.065854 \\ -348.80 & -52.904 & -0.32190 \\ -9.9768 & -6.2822 & 7.6868 \\ -207.41 & -342.04 & 34.068 \end{bmatrix} \begin{bmatrix} x_2 \\ x_3 \\ x_4 \end{bmatrix} + \begin{bmatrix} 1.2407 \\ 5.6584 \\ 656.02 \\ -436.15 \\ -888.74 \end{bmatrix} \tag{7}$$

For the sake of illustration, three sample curves of the proposed correction factor model are plotted in Fig. 7b, and are compared with their corresponding CFD FEM data. The proposed equation has typical relative errors below 5% in range from $0.8cm$ to ∞ and below 10% in range from 0.5 to $0.8cm$.

The proposed equation must be interpreted with caution as its high accuracy is guaranteed only in the aforementioned variable ranges. Note that it physically does not make sense to apply convection formulas for air clearances in range of couple of mm, as the air can be considered almost static due to the viscosity and additional barriers at the top and bottom. In that case, it is suggested that the heat transfer should rather be calculated as conduction through the thin layer of static air between the plate and the semi-enclosure wall. Note that manufacturing tolerances usually do not allow designing of air clearances with less than $2-3mm$ for typical structure sizes encountered in MFTs.

In Fig. 7b, it can be seen that the proposed correction model (6) drastically improves the accuracy of convection formulas, compared to the single plate empirical model.

4. Experimental Verification

In order to verify the proposed formulas, the prototypes of the two geometry details have been realized in such a way to allow measurements in the aforementioned ranges of geometric and thermal variables. Plates were made consisting each out of a heating pad sandwiched between two aluminum plates and two thermal pads. The heating plates are connected to controllable DC sources, where input power P is measured. Thermocouple probes type K were used for temperature measurements. The constructions for models 1 and 2 are displayed in Fig. 8.

For model 1, calculation of the mean convection coefficient on the inside of a plate $\overline{h_1}$ is done via

$$\overline{h_1} = \frac{Q_{conv,i}}{A(T_{si} - T_\infty)} \tag{8}$$

where $Q_{conv,i}$ represents the convection heat dissipation on the inside, A represents the plate side surface area, T_{si} denotes the plate surface temperature on the inside and T_∞ the ambient temperature. Convection heat dissipation on the inside can be calculated as follows:

$$Q_{conv,i} = P - Q_{conv,o} - Q_{rad} \tag{9}$$

where P denotes the measured input power, $Q_{conv,o}$ denotes the convection heat dissipation on the outside of the plate, and Q_{rad} represents the heat dissipation via radiation of the respective plate. Heat dissipation via the upper, lower, front and back surfaces is neglected as the plate width is considered negligible compared to the plate height and length.

ISBN 978-3-8007-5515-8

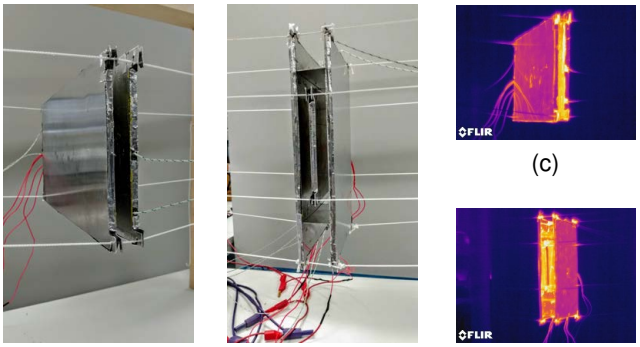

Fig. 8: Experimental setup. Normal view: (a) model 1; (b) model 2; Thermal image: (c) model 1; (d) model 2.

For the convection dissipation on the outside of the plate, empirical equation (1) for convection cooling of a vertical plate in free air is used to determine $\overline{h_o}$ in

$$Q_{conv,o} = \overline{h_o} A (T_{so} - T_\infty) \tag{10}$$

where A is known and T_{so} represents the measured temperature on the outside of the plate.

For the calculation of the heat dissipation by radiation, only the dissipation on the outside of the plate $Q_{rad,o}$ is considered, as the inner side of one plate is exposed to the other parallel plate on the same temperature, resulting in $Q_{rad,i} \approx 0$. $Q_{rad,o}$ is then calculated via

$$Q_{rad,o} = \varepsilon \sigma A (T_{so}^4 - T_\infty^4) \tag{11}$$

where ε represents the emissivity of the objects material and σ the StefanBoltzmann constant. An estimation of ε follows out of a heat dissipation analysis of one heated plate in free air. Out of the difference between input power and convection dissipation calculated via (1), the emissivity of the used aluminum plates is derived, resulting in a value of 0.17, a realistic number for the used aluminum.

Via combination of (8) - (11), the experimental calculation of natural convection coefficients on the inside of parallel plates can be calculated as follows:

$$\overline{h_1} = \frac{P - \overline{h_o} A (T_{so} - T_\infty) - \varepsilon \sigma A (T_{so}^4 - T_\infty^4)}{A (T_{si} - T_\infty)} \tag{12}$$

and, while following a similar strategy, convection

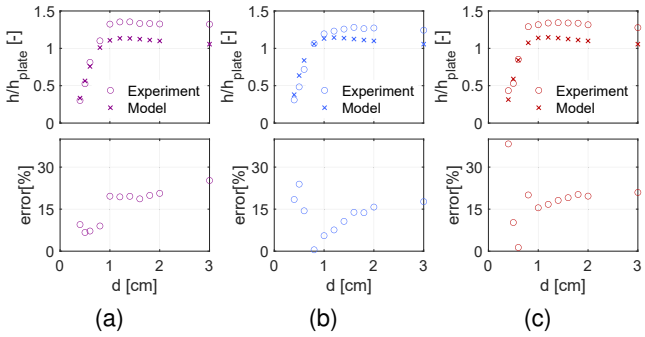

Fig. 9: Comparison of the natural convection correction coefficients, derived from experimental results, with the natural convection correction coefficients, as calculated with proposed correction factor model for model 1, where the experimental data is obtained by changing d with constant input power (a) $P = 14.05W$; (b) $P = 25.50W$; (c) $P = 41.47W$.

Tab. 2: Comparison of the natural convection correction coefficients derived from experimental results $h_{c2,exp}$, with the natural convection correction coefficients, as calculated with proposed correction factor model for model 2 $h_{c2,model}$.

$Exp.$	x_1 $[m]$	x_2 [-]	x_3 [-]	x_4 [%]	$h_{c2,exp}$ [-]	$h_{c2,model}$ [-]	$Error$ [%]
1	0.005	0.48	0.76	85	0.57	0.33	70.3
2	0.005	0.56	0.89	87	0.46	0.27	68.9
3	0.008	0.35	0.55	80	0.94	0.78	20.5
4	0.008	0.47	0.74	63	0.79	0.73	9.16
5	0.008	0.47	0.74	89	0.80	0.64	24.6
6	0.010	0.62	0.98	85	0.71	0.61	16.2
7	0.011	0.44	0.70	72	0.97	0.83	17.9
8	0.013	0.57	0.90	66	0.82	0.76	7.48
9	0.013	0.57	0.90	95	0.84	0.73	15.7
10	0.021	0.40	0.64	78	1.11	0.90	23.7
11	0.021	0.40	0.64	95	1.17	0.89	31.8
12	0.026	0.33	0.52	56	1.13	0.97	16.1
13	0.026	0.33	0.52	95	1.29	0.94	36.4
14	0.026	0.54	0.85	64	0.99	0.82	21.6
15	0.026	0.54	0.85	97	1.05	0.79	31.8

coefficients for the middle plate $\overline{h_2}$ in model 2 can be calculated as follows:

$$\overline{h_2} = \frac{P - 2\varepsilon \sigma A (T_s^4 - T_{s,encl}^4)}{2A (T_s - T_\infty)} \tag{13}$$

A comparison between experimental data and proposed correction factor models are displayed in Fig. 9 and Tab. 2, for models 1 and 2 respectively. As mentioned before, the experimental values $\overline{h_1}$ and $\overline{h_2}$ are divided by the corresponding convection coefficients for a vertical plate in free air, calculated with (1).

In Fig. 9, the experimental data fits the proposed

model remarkably well for small ranges of d, while higher errors appear when the experimental data should converge to 1. This is mainly due to the neglect of radiation dissipation on the inside of the plates, which gets more significant as the plates are further apart. Based on the good correlation of the curves, the value of the derived correction formulas is confirmed, especially in the low air clearance range where the thermal coupling is significant.

Similar trends can be observed in Tab. 2. High relative errors appear for very low d, where the absolute value of h is low and very precise setting of d in the experimental setup is difficult. The increased relative error for high d is again attributed to the underestimation of radiative heat dissipation. Similar as in case of model 1, the validity of the derived correction in model 2 is confirmed.

5. Conclusion

In this work, novel closed-form analytical models have been presented, that capture the effects of the natural air convection cooling within typical MFT geometries, with drastically improved accuracy compared to traditional empirical formulas. They feature accuracy comparable to FEM simulations, yet with negligible computational cost, similar to the traditional empirical formulas. The models have been developed using data driven approach from the results of extensive CFD FEM simulations and successfully verified experimentally within a wide range of geometries.

The proposed models allow efficient and accurate thermal modeling of the MFTs using a thermal network model - where the calculation of the convective thermal resistances is the most challenging part. This enables a very accurate yet computationally efficient and numerically stable thermal design and optimization of the MFT. The use of the computationally intensive CFD FEM simulations can be reduced to final design verification and corrections of various non-modeled details.

References

[1] J. E. Huber and J. W. Kolar, "Solid-State Transformers: On the Origins and Evolution of Key Concepts," *IEEE Industrial Electronics Magazine*, vol. 10, no. 3, pp. 19-28, Sep. 2016.

[2] C. Zhao, D. Dujic, A. Mester, J. K. Steinke, M. Weiss, S. Lewdeni-Schmid, T. Chaudhuri and P. Stefanutti, "Power electronic traction transformer - medium voltage prototype," *IEEE Transactions on Industrial Electronics*, vol. 61, no. 7, pp. 3257-3268, 2014.

[3] M. Claessens et al. "Traction Transformation: A Power-Electronic Traction Transformer (PETT)," *ABB Review, No: 1/12*, pp. 11-17, 2012.

[4] S. Stanisic, M. Jevtic, B. Das, Z. Radakovic. "Fem cfd analysis of air flow in kiosk substation with the oil immersed distribution transformer," FACTA UNIVERSITATIS Series Electronics and Energetics, vol. 31, 2018.

[5] I. Villar. "Multiphysical Characterization of Medium-Frequency Power Electronic Transformers". PhD thesis. EPFL Lausanne, Switzerland, 2010.

[6] G. Ortiz. "High-Power DC-DC Converter Technologies for Smart Grid and Traction Applications". PhD thesis. ETH Zurich, Switzerland, 2014.

[7] M. Bahmani. "Design and Optimization Considerations of Medium-Frequency Power Transformers in High-Power DC-DC Applications". PhD thesis. Chalmers University of Technology Gothenburg, Sweden, 2016.

[8] M. Mogovoric and D. Dujic, "Thermal modeling and experimental verification of an air cooled medium frequency transformer," in *Proceedings of 2017 19th European Conference on Power Electronics and Applications (EPE'17 ECCE Europe)*, Warsaw, 2017, pp. P.1-P.9.

[9] M. Mogorovic and D. Dujic, "FEM-Based Statistical Data-Driven Modeling Approach for MFT Design Optimization," *IEEE Transactions on Power Electronics*, vol. 35, no. 10, pp. 10863-10872, Oct. 2020.

[10] M. Mogorovic and D. Dujic, "Computationally Efficient Estimation of the Electric-Field Maximums for the MFT Insulation Coordination," *IEEE Energy Conversion Congress and Exposition (ECCE)*, Baltimore, MD, USA, 2019, pp. 7118-7123.

[11] S. W. Churchill and H. H. Chu, "Correlating equations for laminar and turbulent free convection from a vertical plate," *International Journal of Heat and Mass Transfer*, vol. 18, no. 11, pp. 1323 - 1329, 1975.